

**Rigorous Criteria for the Collapse of Nonlinear Cooperative Networks**Rui-Jie Wu,<sup>1,\*</sup> Yi-Xiu Kong,<sup>2,\*</sup> Zengru Di,<sup>1</sup> Jordi Bascompte,<sup>3</sup> and Gui-Yuan Shi<sup>1,†</sup><sup>1</sup>Beijing Normal University, 519087 Zhuhai, China<sup>2</sup>Beijing University of Posts and Telecommunications, 100876 Beijing, China<sup>3</sup>University of Zurich, 8057 Zurich, Switzerland

(Received 29 July 2022; accepted 5 February 2023; published 27 February 2023)

Many real-world complex systems, when hitting a tipping point, undergo irreversible sudden shifts that can eventually take a great toll on humanity and the natural world, such as ecosystem collapses, disease outbreaks, etc. Previous work has adopted approximations to predict the tipping points, but due to the nature of nonlinearity, this may lead to unexpected errors in predicting real-world systems. Here we obtain the rigorous bounds of the tipping points for general nonlinear cooperative networks. Our results offer two rigorous criteria that determine the collapse and survival of such a system. These two criteria are decided by the combined effect of dynamical parameters and interaction topology.

DOI: [10.1103/PhysRevLett.130.097401](https://doi.org/10.1103/PhysRevLett.130.097401)

Complex systems often have several different states, in which the whole system behaves differently [1–5]. Predicting tipping points at which the system undergoes irreversible sudden shifts between these states is of great significance. These states are equilibria depending on how the individuals in the system grow, decay, cooperate, and compete with each other. Mathematically, these equilibrium states are fixed points of a set of nonlinear dynamical equations determined by the dynamical parameters and the interaction topology [6].

Typical examples with the potential for tipping points include gene regulatory networks (GRN), where proteins act as activators to produce other proteins, epidemiology, where people spread a disease to each other, and plant-animal mutualistic networks, where plants provide food to their animal partners in exchange for pollination or seed dispersal services [7]. In the latter case, mutualistic networks involve dozens or even hundreds of species belonging to two groups: plants and animals, with species in the same group competing with each other and species from different groups benefiting from each other. Models of mutualistic ecological networks are highly complex, and previous work on the resilience of these systems and their likelihood to undergo a tipping point have relied on numerical simulations [8,9].

Thereupon, some studies focus on some simplified models without considering the competition within each group. For example, Gao *et al.* [10] assume that all

regulations are activation type in GRNs; Morone *et al.* [11] studied a simplified plant-pollinator network model with only self-decay and cooperation; in the susceptible-infected-susceptible (SIS) model, the infection of others does not reduce one's probability of being infected, etc.

We use the general term cooperative networks to refer to such models. In these models, equilibria of the system are the result of the combined effect of growth, decay and cooperation. However, even without the competition term, the complex topology of the interacting network and nonlinear dynamics still poses a great difficulty. Scientists seeking tipping points have to adopt approximations, such as using mean-field approximation [12], second-order mean field under quasilinear assumption [10], step function approximation [11], and Taylor expansion [13]. But as is suggested by the famous butterfly effect [14], nonlinearity indicates that even tiny approximations may cause unexpected error in the prediction.

With the risk of unexpected errors, people are concerned when these predictions can be correctly applied [15,16], so rigorous results are still in dire need. In this Letter, we obtain the first rigorous bounds of the tipping points for general cooperative networks. Our theoretical results guarantee the survival and collapse of general cooperative networks, with arbitrary dynamical form and arbitrary interaction topology.

For a system consisting of components interacting with each other through a given interaction topology, with component nodes  $i, j, \dots$ , the cooperative dynamics can be described by the following set of differential equations:

$$\frac{dx_i}{dt} = F\left(x_i, \sum_{j=1}^N A_{ij}G(x_i, x_j)\right), \quad (1)$$

Published by the American Physical Society under the terms of the [Creative Commons Attribution 4.0 International license](https://creativecommons.org/licenses/by/4.0/). Further distribution of this work must maintain attribution to the author(s) and the published article's title, journal citation, and DOI.

where  $A_{ij}$  is the adjacency matrix of the interaction network.  $A_{ij} > 0$  if component  $j$  interacts with component  $i$ , otherwise  $A_{ij} = 0$ . One can choose an appropriate function  $F$  so as to represent different cooperative dynamics (examples are shown in Table I). Note that this model can represent many cooperative systems that have weighted or directed interaction networks, including systems with self-edges. For instance, in GRNs, interaction strength can be described by the weights of edges, unidirectional interaction can be represented by directed edges, a promoter can promote the generation of its own products, and the form of the dynamical functions stays unchanged in such cases.

The equations describe the dynamics of each component  $i$ . Here the second term  $u_i = \sum_{j=1}^N A_{ij}G(x_i, x_j)$  represents the total incoming interactions (all supportive effects in cooperative systems) the component  $i$  receives from its neighbors in the complex network. Here we study dynamical systems that satisfy the following conditions: (1)  $F(\mathbf{x} = \mathbf{0}) = 0$  and  $\lim_{\|\mathbf{x}\| \rightarrow +\infty} d\|\mathbf{x}\|/dt < 0$ : the components' abundance values do not grow out of nothing and cannot grow to infinity. (2)  $F(x_i > 0, u_i = 0) < 0$ : the components spontaneously self-decay. (3)  $\partial F/\partial u_i \geq 0$ : the incoming interactions support the survival of the components. (4)  $\partial G/\partial x_j \geq 0$ ,  $G(x_i, 0) = 0$ : higher abundance of a neighboring component means stronger support.

Among them, conditions 1 and 2 are generally true for many dynamical systems originating from natural processes, and they guarantee the system has no trivial nonzero states. Because if a system does not satisfy conditions 1 and 2, it may have a nonzero solution even if there are no cooperative dynamics. Meanwhile, the cooperative dynamics we focus on in this Letter are represented by conditions 3 and 4. These two conditions guarantee that the interactions from the network can support the survival of a component, and further result in positive feedback loops, enhancing nonlinear dynamics in the system. Now, the key question is, in this cooperative model, under what

environment will such systems collapse, i.e., under what circumstances does the system have a nonzero fixed point?

In a nutshell, the final state of a system is the result of conflicting interactions between two effects: the self-decaying effect and the incoming supports from the network. We can imagine that a difficult environment would cause self-decay to be too fast, or support to be insufficient, meaning that the whole system can only stay in the zero-abundance state. However, increasing the connectivity or coupling strength in the underlying complex network may allow the system to survive (fixed point at nonzero abundance). The self-decay term is only related to parameters in the dynamical equations, while the incoming cooperative supports are related to both the interaction topology and the dynamics.

To obtain the rigorous bounds of tipping points, our idea is to study the sufficient or necessary conditions for the original heterogenous system to have a nonzero fixed point. In simple terms, one needs to find simple hypothetical systems, which are analytically solvable systems, that are strictly more fragile or robust than the original system. The first key question is what network topology allows the dynamical equation to be solved analytically. The most straightforward answer to that is a symmetrical network, in which all nodes are identical to each other. The tipping points of this hypothetical system can be solved easily. Compared with the original heterogenous system, the heterogeneity of the original networks will induce an uncertainty to the tipping points of this hypothetical symmetrical system. But the maximum boundaries of uncertainty are strictly bounded by mathematical properties of the network structure. In the case of a symmetrical network, we can replace  $x_i, x_j$  with  $x$  and  $\sum_j A_{ij}$  with  $\lambda$ , then the fixed-point solution of Eq. (1) becomes the following one-variable equation:

$$F(x, \lambda G(x, x), \alpha, \beta, \gamma \dots) = 0. \quad (2)$$

TABLE I. Summary of three cooperative systems analyzed in this Letter. GRN consists of a set of interactions of proteins in the cell to control the gene expression levels of activators.  $x_i \geq 0$  is the concentration of activator  $i$ . The first term determines the degradation and  $B$  is the degradation rate, whereas the parameter  $h$  is the Hill coefficient that quantifies cooperativity of the gene regulation [10,17]. A mutualistic network such as that relating plants and their insect pollinators is a system where the survival of species benefits from the survival of other species.  $x_i \geq 0$  is the abundance of species  $i$ ,  $d \geq 0$  is the death rate,  $s > 0$  is a self-limitation parameter,  $\alpha > 0$  is the half-saturation constant, and  $\gamma > 0$  is the mutualistic interaction efficiency [11]. Susceptible-infected-susceptible epidemic process model consists of two types of nodes: susceptible ( $S$ ) or infected ( $I$ ). Susceptible can become infected through a direct contact with an infected, while the infected can recover and become susceptible again. Here  $0 \leq x_i \leq 1$  is the probability that node  $i$  is infected,  $\beta > 0$  is the infection rate [18].

Model	Equation	$F(x_i, u_i)$	$G(x_i, x_j)$
GRN	$(dx_i/dt) = -Bx_i + \sum_{j=1}^N A_{ij}[x_j^h/(1+x_j^h)]$	$-Bx_i + u_i$	$x_j^h/(1+x_j^h)$
Plant-pollinator network	$(dx_i/dt) = -x_i d - x_i^2 s + [(\gamma \sum_{j=1}^N A_{ij} x_j)/(\alpha + \sum_{j=1}^N A_{ij} x_j)]x_i$	$-x_i d - x_i^2 s + [\gamma u_i/(\alpha + u_i)]x_i$	$x_j$
SIS epidemic process	$(dx_i/dt) = -x_i + \beta \sum_{j=1}^N A_{ij}(1-x_i)x_j$	$-x_i + \beta u_i$	$(1-x_i)x_j$

For convenience, we use  $S(\lambda)$  to represent a symmetric network whose weighted in-degree equals  $\lambda$ . Given environment parameters  $(\alpha, \beta, \gamma, \dots)$ , we calculate  $\lambda^*$  as a function of  $(\alpha, \beta, \gamma, \dots)$ , which is the minimal value of  $\lambda$  that allows  $S(\lambda)$  to survive, i.e., allows Eq. (2) to have at least one positive solution. To assist intuitive understanding, we interpret  $\lambda^*$  as the effective difficulty of the environment, see Fig. 1 for illustration. As we proved in the Supplemental Material [19],  $S[k_{\max}(A)]$  is strictly more fragile (see Proposition 1 in the Supplemental Material [19]) and  $S[\rho(A)]$  is strictly more robust (see Proposition 2 in Supplemental Material [19]) than the original heterogeneous network, respectively. This result offers us two simple and easily applicable criteria: (1) If  $\lambda^* \leq k_{\max}(A)$ , the heterogeneous system will survive; (2) if  $\lambda^* \geq \rho(A)$ , the heterogeneous system will collapse. [The second criterion does not stand when  $G(x_i, x_j) \neq f(x_i) \cdot g(x_j)$ ; we present such an example in Proposition 3 in the Supplemental Material [19].]

This also means that all the tipping points of the system must fall into the region  $k_{\max}(A) \leq \lambda^* \leq \rho(A)$ .  $k_{\max}(A)$  is the maximum  $k$  coreness of the weighted network [23–25], defined as the maximum number that allows the existence of a subgraph in which each node receives at least  $k_{\max}(A)$  weighted incoming edges in total within the subgraph; and  $\rho(A)$  is the largest eigenvalue of  $A$ . In the following,  $\rho(A)$  and  $k_{\max}(A)$  are referred to as  $\rho$  and  $k_{\max}$ , respectively.

Furthermore, we prove that if one wants to obtain the upper and lower bounds that are universally available to the general nonlinear cooperative system,  $k_{\max}$  and  $\rho$  are the infimum (the greatest lower bound) and supremum (the lowest upper bound) of the tipping points, respectively. The supremum of tipping points  $\lambda^* = \rho$  can be reached when

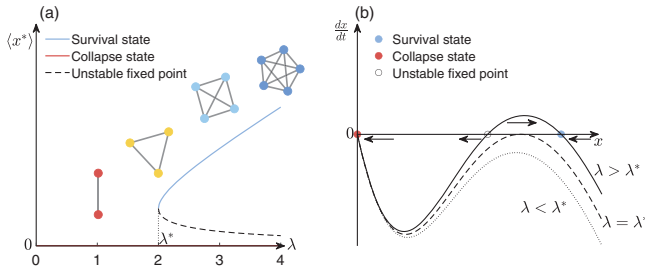


FIG. 1. Illustrations of effective difficulty  $\lambda^*$  and stability of a dynamical system. (a) Gauge of environment difficulty using a series of symmetric networks. Red line indicates collapse state of the system, while blue line indicates survival state of the system. Note that  $\lambda^*$  is not necessarily an integer, since edges of networks can be weighted, and a symmetric network is not necessarily a fully connected network. (b) Emergence of a nonzero fixed point when we increase  $\lambda$ . This corresponds to the emergence of a survival state at  $\lambda^*$  in (a). The red dot in the horizontal axis represents the collapse state; the blue dot represents the survival state; black circle shows an unstable fixed point; and dotted, dashed, and solid lines show the dynamical function when  $\lambda$  increases.

the corresponding symmetric system described by Eq. (2) undergoes a continuous transition (see Proposition 4 in the Supplemental Material for details [19]). Here, interestingly, the tipping points are free of dynamical forms, meaning that even though the dynamics are unknown, the system can be controlled effectively through changing the network topology in a way that causes the largest change in  $\rho(A)$ . The infimum  $\lambda^* = k_{\max}$  can be reached when  $G(x_i, x_j)$  is a step function of  $x_j$ , which is a commonly used method in theoretical studies [11,17].

Later we will show through numerical simulations that existing predictions are likely to misjudge the fate of the system, and the tipping points sometimes even fall beyond the rigorous boundaries. This is probably due to the nature of the nonlinearity that adopting approximations may cause unexpected errors in predictions. To simplify the applications, we provide the following simple scheme to assist the analysis from diverse backgrounds: (1) The first step is to obtain the one-variable fixed-point equation as Eq. (2) from the original dynamical equation. (2) The second step is to obtain the environmental difficulty  $\lambda^*$  as a functional form of dynamical parameters conditioned by Eq. (2). In this case, the left-hand side of Eq. (2)  $F(x, \lambda G(x, x), \alpha, \beta, \gamma, \dots)$  must satisfy simultaneous equations  $F = 0$  and  $dF/dx = 0$ , then  $\lambda^*$  can be solved. (3) Step 3 is to apply our two criteria to the heterogeneous system. To be more specific, if it is a favorable system, ensure that it runs in the region where  $\lambda^* \leq k_{\max}$ , so to guarantee the survival; otherwise, we make the system stay in the region where  $\lambda^* \geq \rho$  to ensure the collapse.

In the following, we show numerical simulations for the three models introduced in Table I. These results also serve as exemplar protocols for the analysis of general nonlinear cooperative systems.

**GRNs.**—First let us consider the example of GRNs [10]. To study such a heterogeneous system, the first step is to rewrite the dynamical equation into a one-variable fixed-point equation like Eq. (2),

$$-Bx + \lambda \frac{x^h}{1 + x^h} = 0. \quad (3)$$

Obviously, when  $h < 1$ , a positive solution always exists, because the left-hand side is always larger than zero when  $x \rightarrow 0$ . When  $h \geq 1$ , the effective difficulty  $\lambda^*$  is the minimal  $\lambda$  that allows for positive  $x$ . We apply step 2 of the scheme and obtain

$$\lambda^* = Bh(h-1)^{\frac{1}{h}-1}. \quad (4)$$

Here  $h$  is fixed by the details of the biological regulation, whereas  $B$  changes depending on external stress and living conditions. Applying our criteria, given a real heterogeneous network, we can assert the following: (1) In the region  $\lambda^* \leq k_{\max}$ , i.e.,  $B \leq k_{\max}/[h(h-1)^{(1/h)-1}]$ , the activators

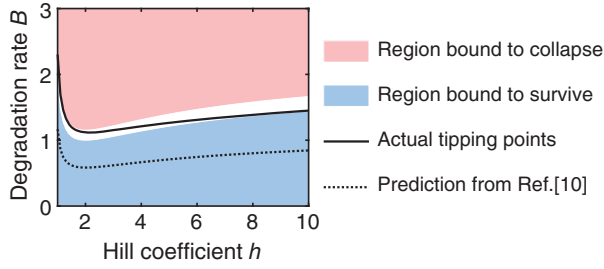


FIG. 2. The phase diagram of a GRN. The red and blue areas show the collapse region where  $\lambda^* \geq \rho$  and the survival region where  $\lambda^* \leq k_{\max}$ , respectively. The solid line shows actual tipping points obtained by numerical simulations on a real *E. coli* network. The dotted line shows tipping points predicted from Ref. [10].

have positive concentrations, and the transcriptional regulation process works. (2) In the region  $\lambda^* \geq \rho$ , i.e.,  $B \geq \rho/[h(h-1)^{(1/h)-1}]$ , the concentration of all the activators fall to zero.

Fixing parameter  $h$ , for each  $B$ , we can obtain the corresponding average abundance of the original complex system  $\langle \mathbf{x}^* \rangle$  through numerical simulations and then find the tipping point  $(h, B)$  at which the corresponding  $\langle \mathbf{x}^* \rangle$  just collapses to zero. A numerical simulation on a GRN for *E. coli* [26] is shown in Fig. 2. The actual tipping points (solid line) lie in the gap between our collapse region (red) and survival region (blue), showing our results are correct.

It can be seen that the tipping point changes with the onset of nonlinearity. The solid line slowly approaches the blue border  $\lambda^* = k_{\max}$  [when  $h \rightarrow +\infty$ ,  $G(x_i, x_j)$  is a step function of  $x_j$ ] from the red border  $\lambda^* = \rho$  [when  $h = 1$ , the symmetric system described by Eq. (3) undergoes a continuous transition]. As a comparison, we also plot the state-of-the-art prediction of tipping points by Ref. [10] (dotted line).

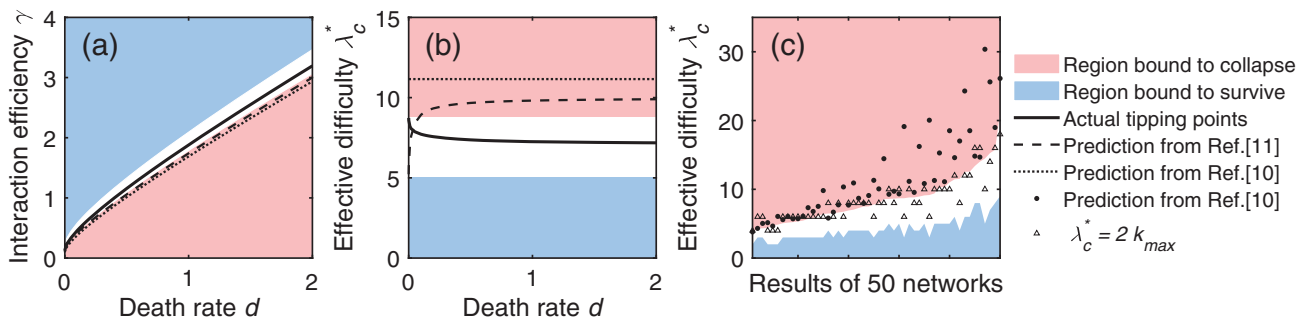


FIG. 3. Tipping points in a mutualistic network of species interactions. Similar to Fig. 2, the solid line shows the actual tipping points obtained from numerical simulations. Red and blue areas show the collapse region where  $\gamma \leq (\sqrt{\alpha s/\rho} + \sqrt{d})^2$  and the survival region where  $\gamma \geq (\sqrt{\alpha s/k_{\max}} + \sqrt{d})^2$ , respectively. The dotted line shows tipping points predicted in Ref. [10], and the dashed line shows the prediction from Ref. [11]. (a) The phase diagram of a pollination network of the spring wildflower community in the deciduous forests of the Piedmont region in North Carolina, which contains 57 species and 143 interactions. (b) The dependence of  $\lambda_c^*$  on parameter  $d$  of the same network, where  $\lambda_c^*$  can be calculated from Eq. (6). (c) Results of 50 real pollination networks. Horizontal axis marks the 50 networks, and for each network the prediction of tipping points from Ref. [10] is shown by black dots and  $2k_{\max}$  is shown by triangles (Ref. [11] predicts  $\lambda_c^*$  increases from  $k_{\max}$  to  $2k_{\max}$  as  $d$  increases). The networks are ranked by an increasing order of theoretical upper bound of tipping points, i.e., the largest eigenvalue of the networks.

*Plant-pollinator network.*—Next, we study the plant-pollinator network we briefly introduced in Table I. Although these systems have been described by a set of differential equations containing both the cooperative term between sets and the interspecific competition term within sets [27], here we omit the latter for the sake of analytical treatment as in Ref. [11]. The corresponding one-variable equation of such systems is

$$-xd - x^2s + \frac{\gamma\lambda x^2}{\alpha + \lambda x} = 0, \quad (5)$$

which has an effective environment difficulty

$$\lambda^* = \frac{\alpha s}{(\sqrt{\gamma} - \sqrt{d})^2}. \quad (6)$$

Applying the criteria, we obtain the following conclusions for heterogenous plant-pollinator networks: (1) If  $\lambda^* \leq k_{\max}$ , i.e.,  $\gamma \geq (\sqrt{\alpha s/k_{\max}} + \sqrt{d})^2$ , the species can coexist. (2) If  $\lambda^* \geq \rho$ , i.e.,  $\gamma \leq (\sqrt{\alpha s/\rho} + \sqrt{d})^2$ , all species go extinct.

For  $d = 0$ , the one-variable system described by Eq. (5) undergoes a continuous transition; this shows the original heterogenous system has a continuous transition around  $\rho(A) = \alpha s/\gamma$ . Meanwhile, when  $d > 0$ , the system undergoes a discontinuous transition. Here the tipping points form a hypersurface in four-dimensional space. In Figs. 3(a) and 3(b), we show the results on a pollination network (see Fig. 3 for detailed description). To better illustrate this surface on a 2D graph, we fix  $s = 1$  and  $\alpha = 1$  (one can choose to fix other parameters) and plot the tipping point  $\gamma^*$  in Fig. 3(a) and its corresponding effective difficulty  $\lambda_c^*$  in Fig. 3(b) as function of parameter  $d$  from 0 to 2.

To compare with existing state-of-the-art predictions by Refs. [10,11] more clearly, we calculate two  $\lambda_c^* = \alpha s / (\sqrt{\gamma^*} - \sqrt{d})^2$ , predicted by the two methods. Then we plot  $\lambda_c^*$  as functions of parameter  $d$  from 0 to 2; here  $\gamma^*$  represents the critical value of  $\gamma$  as a function of  $d$  when we fix  $s = 1$  and  $a = 1$ . As shown in Fig. 3,  $\lambda_c^*$ , corresponding to actual tipping points [solid lines in Figs. 3(a) and 3(b)], decreases from  $\rho$  and stays larger than  $k_{\max}$  as  $d$  increases, as we predicted. The results in Ref. [11] [dashed lines in Figs. 3(a) and 3(b)] indicate that  $\lambda_c^*$  increases from  $k_{\max}$  to  $2k_{\max}$ . This means when  $d$  is small, the risk for the network to collapse will be overestimated; when  $d$  is large, the risk will be underestimated. These systematic biases are also observed in the original Fig. 2(g) in Ref. [11]. Meanwhile, it can be seen from Figs. 3(a) and 3(b) that the tipping points predicted in Ref. [10] fall into the collapse region, indicating an underestimation of the collapse risk. This is probably due to the existence of a large hub or unbalanced sizes of the two parties. An extreme case is the star network, where Ref. [10] predicts the tipping points  $\lambda_c^* = N/2$ , which are much larger than the actual upper bound  $\rho = \sqrt{N-1}$ . To further validate our analysis, in Fig. 3(c), we tested 50 real pollination networks from Web of Life, and the results support the above analysis.

*Epidemic process.*—The corresponding one-variable equation of the SIS model is  $-x + \lambda\beta(1-x)x = 0$ , which leads to  $\lambda^* = 1/\beta$ . The symmetric system undergoes a continuous transition, thus we predict the original heterogeneous system has a continuous transition near  $\beta \times \rho = 1$ , which is in agreement with a previous study [18,28].

In conclusion, for general nonlinear cooperative systems, albeit simple enough, our theorem gives the rigorous bounds of tipping points [ $k_{\max}(A)$  and  $\rho(A)$ , respectively]. These bounds are universal, and results do not depend on the specific form of the dynamical equations and the interaction network topology. These bounds provide two useful criteria to determine the final state of a heterogeneous system: the system can always survive when the difficulty of the environment  $\lambda^* \leq k_{\max}(A)$ ; and it will always collapse when  $\lambda^* \geq \rho(A)$ . It is important to note that our approach has made simplifying assumptions, chiefly the lack of competition within sets. Future work should explore to what degree our results stand when departing from those assumptions. Still, our findings open the door to accurately assessing the likelihood of ecological communities collapsing in the face of global environmental change, gene regulation networks malfunctioning in the face of mutation, or infectious diseases being eradicated through public health intervention.

Datasets for Figs. 2 and 3 are publicly available at [29,30], respectively.

We thank Kim Sneppen for inspiring discussions on gene regulatory networks. This work has received funding from the National Science Foundation of China (NSFC) (Grant

No. 71731002), the European Research Council (ERC) under the European Union's Horizon 2020 Research and Innovation Program (Grant No. 740704), and Research Funds for the Central Universities from the Beijing University of Posts and Telecommunications (Grant No. 505022019).

\*R.-J. W. and Y.-X. K. contributed equally to this work.

†sgy@bnu.edu.cn

- [1] M. Scheffer, S. Carpenter, J. A. Foley, C. Folke, and B. Walker, *Nature (London)* **413**, 591 (2001).
- [2] M. Scheffer, J. Bascompte, W. A. Brock, V. Brovkin, S. R. Carpenter, V. Dakos, H. Held, E. H. Van Nes, M. Rietkerk, and G. Sugihara, *Nature (London)* **461**, 53 (2009).
- [3] R. P. Rohr, S. Saavedra, and J. Bascompte, *Science* **345** (2014).
- [4] B. M. Arani, S. R. Carpenter, L. Lahti, E. H. Van Nes, and M. Scheffer, *Science* **372**, eaay4895 (2021).
- [5] G. Ambika and J. Kurths, *Tipping in complex systems: Theory, methods and applications*, *Eur. Phys. J. Spec. Top.* **230**, 3177 (2021).
- [6] S. H. Strogatz, *Nonlinear Dynamics and Chaos with Student Solutions Manual: With Applications to Physics, Biology, Chemistry, and Engineering* (CRC Press, Boca Raton, 2018), 10.1201/9780429492563.
- [7] J. Bascompte and P. Jordano, *Mutualistic Networks* (Princeton University Press, Princeton, NJ, 2013), 10.23943/princeton/9780691131269.001.0001.
- [8] J. J. Lever, E. H. van Nes, M. Scheffer, and J. Bascompte, *Ecol. Lett.* **17**, 350 (2014).
- [9] V. Dakos and J. Bascompte, *Proc. Natl. Acad. Sci. U.S.A.* **111**, 17546 (2014).
- [10] J. Gao, B. Barzel, and A.-L. Barabási, *Nature (London)* **530**, 307 (2016).
- [11] F. Morone, G. Del Ferraro, and H. A. Makse, *Nat. Phys.* **15**, 95 (2019).
- [12] R. Pastor-Satorras and A. Vespignani, *Phys. Rev. Lett.* **86**, 3200 (2001).
- [13] E. Laurence, N. Doyon, L. J. Dubé, and P. Desrosiers, *Phys. Rev. X* **9**, 011042 (2019).
- [14] E. N. Lorenz, *J. Atmosph. Sci.* **20**, 130 (1963).
- [15] P. Kundu, H. Kori, and N. Masuda, *Phys. Rev. E* **105**, 024305 (2022).
- [16] C. Tu, J. Grilli, F. Schuessler, and S. Suweis, *Phys. Rev. E* **95**, 062307 (2017).
- [17] U. Alon, *An Introduction to Systems Biology: Design Principles of Biological Circuits* (Chapman and Hall/CRC, New York, 2019), 10.1201/9780429283321.
- [18] R. Pastor-Satorras, C. Castellano, P. Van Mieghem, and A. Vespignani, *Rev. Mod. Phys.* **87**, 925 (2015).
- [19] See Supplemental Material at <http://link.aps.org/supplemental/10.1103/PhysRevLett.130.097401> for the proofs and explanation of the theorems in the main text, which includes Refs. [20–22].
- [20] A. Berman and R. J. Plemmons, *Nonnegative Matrices in the Mathematical Sciences* (SIAM, Philadelphia, 1994).
- [21] L. Collatz, *Math. Z.* **48**, 221 (1942).
- [22] H. Wielandt, *Math. Z.* **52**, 642 (1950).

- [23] M. Eidsaa and E. Almaas, *Phys. Rev. E* **88**, 062819 (2013).
- [24] Y.-X. Kong, G.-Y. Shi, R.-J. Wu, and Y.-C. Zhang, *Phys. Rep.* **843**, 1 (2019).
- [25] R.-J. Wu, Y.-X. Kong, Z. Di, Y.-C. Zhang, and G.-Y. Shi, *Physica A* **608**, 128260 (2022).
- [26] S. Gama-Castro, V. Jiménez-Jacinto, M. Peralta-Gil, A. Santos-Zavaleta, M. I. Peñaloza-Spinola, B. Contreras-Moreira, J. Segura-Salazar, L. Muniz-Rascado, I. Martínez-Flores, H. Salgado *et al.*, *Nucl. Acids Res.* **36**, D120 (2008).
- [27] U. Bastolla, M. A. Fortuna, A. Pascual-García, A. Ferrera, B. Luque, and J. Bascompte, *Nature (London)* **458**, 1018 (2009).
- [28] A. Lajmanovich and J. A. Yorke, *Math. Biosci.* **28**, 221 (1976).
- [29] J. Gao, Version 2.0 (2018), <https://github.com/jianxigao/NuRsE>.
- [30] R. Ortega, M. A. Fortuna, and J. Bascompte, <https://www.web-of-life.es/>.